Piitulainen, Harri; Bourguignon, Mathieu; De Tiege, Xavier; Hari, Riitta; Jousmäki, Veikko

# Corticokinematic coherence during active and passive finger movements

*Published in:*
Neuroscience

*DOI:*
10.1016/j.neuroscience.2013.02.002

Published: 01/01/2013

*Document Version*
Publisher's PDF, also known as Version of record

*Neuroscience* 238 (2013) 361–370

# CORTICOKINEMATIC COHERENCE DURING ACTIVE AND PASSIVE FINGER MOVEMENTS

**H. PIITULAINEN,** [a*†] **M. BOURGUIGNON,** [a,b†] **X. DE TIÈGE,** [b] **R. HARI** [a,c] **AND V. JOUSMÄKI** [a,b]

[a] *Brain Research Unit, O.V. Lounasmaa Laboratory and MEG Core, Aalto NeuroImaging, School of Science, Aalto University, P.O. Box 15100, FI-00076 AALTO, Espoo, Finland*

[b] *Laboratoire de Cartographie Fonctionnelle du Cerveau, ULB-Hôpital Erasme, 808 Lennik Street, B-1070 Bruxelles, Belgium*

[c] *Advanced Magnetic Imaging Centre, Aalto NeuroImaging, School of Science, Aalto University, P.O. Box 13000, FI-00076 AALTO, Espoo, Finland*

**Abstract—Corticokinematic coherence (CKC) refers to coupling between magnetoencephalographic (MEG) brain activity and hand kinematics. For voluntary hand movements, CKC originates mainly from the primary sensorimotor (SM1) cortex. To learn about the relative motor and sensory contributions to CKC, we recorded CKC from 15 healthy subjects during *active* and *passive* right index-finger movements. The fingertip was either touching or not touching table, resulting in *active-touch*, *active-no-touch*, *passive-touch*, and *passive-no-touch* conditions. The kinematics of the index-finger was measured with a 3-axis accelerometer. Beamformer analysis was used to locate brain activations for the movements; somatosensory-evoked fields (SEFs) elicited by pneumatic tactile stimulation of the index finger served as a functional landmark for cutaneous input. All *active* and *passive* movements resulted in statistically significant CKC at the movement frequency (F0) and its first harmonic (F1). The main CKC sources at F0 and F1 were in the contralateral SM1 cortex with no spatial differences between conditions, and distinct from the SEF sources. At F1, the coherence was by two thirds stronger for *passive* than *active* movements, with no difference between *touch vs. no-touch* conditions. Our results suggest that the CKC occurring during repetitive finger movements is mainly driven by somatosensory, primarily proprioceptive, afferent input to the SM1 cortex, with negligible effect of cutaneous input.**



**Key words: acceleration, human brain, magnetoencephalography, proprioception, sensorimotor cortex.**

## INTRODUCTION

Kinematics of repetitive executed and observed hand movements is coherent with magnetoencephalographic (MEG) brain activity both at the movement frequency (F0) and its first harmonic (F1) (Jerbi et al., 2007; Bourguignon et al., 2011, 2012, 2013b; Piitulainen et al., 2013). The cortical sources of this corticokinematic coherence (CKC) are located in the contralateral primary sensorimotor (SM1) cortex. However, the relative motor and sensory contributions to CKC in the context of self-executed hand movements are still unknown. One approach to unravel these contributions is to compare CKC under *active vs. passive* movements and to vary the level of cutaneous tactile input. During passive movements, the effect of corticospinal efferents is negligible while movement-related afferent somatosensory information is preserved.

According to single-neuron recordings, both the primary motor (M1) and primary somatosensory (S1) cortices receive proprioceptive feedback, and certain human M1 neurons discharge during both active and passive hand movements while remaining silent during tactile stimulation (Goldring and Ratcheson, 1972). In neuroimaging studies, both active and passive upper limb (hand and elbow) movements may result in strikingly similar activation patterns in the contralateral SM1 cortex, covering both the M1 and S1 cortices (positron emission tomography, PET, (Weiller et al., 1996); functional magnetic resonance imaging fMRI, (Reddy et al., 2001; Kocak et al., 2009)). According to MEG recordings, passive finger and toe movements activate S1 and secondary somatosensory cortices, but the results have been more diverse on M1 involvement (Xiang et al., 1997a,b; Mima et al., 1999; Alary et al., 2002; Woldag et al., 2003).

We aimed to disentangle motor and sensory contributions to CKC by (1) comparing coherence strength during continuous *active* and *passive* right index-finger movements, (2) comparing the cortical source locations between *active* and *passive* movements and with respect to the sources of somatosensory-evoked fields (SEFs), and (3) evaluating the effect of tactile input on coherence. We hypothesized that cortical CKC sources would be more

*Corresponding author. Tel: +358-505-680-654; fax: +358-9-470-22969.
E-mail address: harri.piitulainen@aalto.fi (H. Piitulainen).
† These authors equally contributed to this work.

*Abbreviations:* CKC, corticokinematic coherence; DICS, dynamic imaging of coherent sources; EMG, electromyography; F0, movement frequency of finger movements; fMRI, functional magnetic resonance imaging; F1, first harmonic of finger movement frequency; M1 cortex, primary motor cortex; MRIs, magnetic resonance images; MEG, magnetoencephalography; MNI brain, standard Montreal Neurological Institute brain; PET, positron emission tomography; S1 cortex, primary somatosensory cortex; SM1, primary sensorimotor cortex; SEF, somatosensory-evoked field; SEP, somatosensory-evoked potential.

0306-4522/13 
http://dx.doi.org/10.1016/j.neuroscience.2013.02.002

posterior for *passive* than *active* movements due to a posterior shift of the center of gravity of SM1 activation because of decreased motor–cortex involvement (Reddy et al., 2001). Furthermore, by varying the amount of tactile input (the moved finger either touching or not touching the table supporting the hand), we attempted to locate CKC sources with respect to S1 index-finger area, indentified by tactile SEFs. Finally, we expected the strength of CKC in different conditions to inform about the relative motor and sensory contributions.

## EXPERIMENTAL PROCEDURES

### Subjects

Fifteen healthy subjects (mean age 29.4 yrs, range 21–38; 8 males, 7 females) without any history of neuropsychiatric disease or movement disorders were studied. According to Edinburgh handedness scale (Oldfield 1971), 14 subjects were right-handed (mean 92, range 67–100; left–right scale from −100 to +100) and one subject was ambidextrous (−20).

The study had a prior approval by the ethics committee of the Helsinki and Uusimaa district, and the subjects gave written informed consent before participation. Subjects were compensated monetarily for the lost working hours and travel expenses.

### Experimental protocol

During MEG recordings, subjects sat with the left hand on the thigh and the right hand on a table positioned in front of them. Earplugs were used to reduce concomitant auditory noise. Subjects were instructed to fixate a self-chosen detail in a picture ($21 \times 30\ cm^2$) on the wall of the magnetically shielded room, positioned 2.8 m in front of them, 11 deg to the left from the midline. A white paper sheet taped vertically on the MEG gantry prevented the subjects from seeing their right hand moving.

Subjects underwent six experimental conditions (four movement conditions, SEFs to tactile stimulation, and a *rest* condition). The order of the six conditions was randomized for each subject. The four movement conditions (*active-touch*, *active-no-touch*, *passive-touch*, and *passive-no-touch*) involved continuous flexion–extension of the right index-finger at a frequency around 4 Hz for 3.5 min, and they comprised two movement tasks, *active* and *passive*, and two movement types, *touch* and *no-touch*. The finger movements occurred mainly at the metacarpophalangeal joint. In *touch* conditions, the tip of the index finger touched the table whereas in *no-touch* conditions it did not. Subject performed the *active* movements with a self-paced rate. In the *passive* task, the investigator moved a light aluminum stick, attached with Velcro strap to the middle segment of the subjects right index-finger, with a self-paced rate around 4 Hz (Fig. 1, right). To reduce cutaneous stimulation during passive movements, the middle phalanx of the index finger was covered with surgical paper tape prior to the placement of the Velcro strap. Subjects did not see the investigator who sat on the right side behind the paper screen.

The kinematics of the right index-finger was monitored with a 3-axis accelerometer (ADXL335 iMEMS Accelerometer, Analog Devices, Inc., Norwood, MA, USA) attached to the index-finger nail (Fig. 1). The accelerometer did not produce artifacts to the MEG signals.

For SEF recordings, tactile pneumatic stimuli (duration 183 ms, peak at 36 ms) were delivered to subject's right fingertip once every 500 ms, for 4 min, which resulted in about 480 stimuli.

In the *rest* condition, carried out for noise estimation, subjects rested eyes open during 3.5 min.

### Measurements

*MEG.* The measurements were carried out at the MEG Core of the Brain Research Unit, Aalto University. Cerebral activity was recorded in a magnetically shielded room (Imedco AG, Hägendorf, Switzerland) with a 306-channel whole-scalp neuromagnetometer (Elekta Neuromag™, Elekta Oy, Helsinki, Finland). The recording passband was 0.1–330 Hz and the signals were sampled at 1 kHz. The subject's head position inside the MEG helmet was continuously monitored by feeding current to four head-tracking coils located on the scalp. The locations of the coils with respect to anatomical fiducials were determined with an electromagnetic tracker (Fastrak, Polhemus, Colchester, VT, USA). Co-registration with the MRI images was based on three anatomical fiducials and additional digitization points.

*Acceleration and EMG.* Accelerometer and surface electromyographic (EMG) signals were recorded time-locked to MEG signals, low-pass filtered at 330 Hz and sampled at 1 kHz (Fig. 1). EMG electrodes were placed in bipolar configuration (impedance < 10 kΩ) with 20-mm inter-electrode distance over *extensor digitorum* and *flexor carpi radialis* muscles. A ground electrode was placed on left side of the subject's neck.

*MRI.* 3D-T1 magnetic resonance images (MRIs) were acquired with whole-body General Electric Signa® VR 3.0T MRI scanner (Signa VH/i, General Electric, Milwaukee, WI) at the AMI Centre of the Aalto University.

### Data processing

*MEG and MRI pre-processing.* Continuous MEG data were pre-processed off-line using the signal-space-separation (SSS) method to suppress external interferences, correct for head movements, and align head positions across the sessions (Taulu et al., 2004). The signals were band-pass filtered through 1–195 Hz off-line and epochs exceeding 3 pT (magnetometers) or 0.7 pT/cm (gradiometers) were excluded to avoid contamination by eye movements, muscle activity, and artifacts in MEG sensors. Individual MRIs were segmented using Freesurfer software (Martinos Center for Biomedical Imaging, Massachusetts, USA). Then, the MEG forward model for two orthogonal tangential current dipoles was computed for each node of a 5-mm mesh of the white–gray matter interface using MNE suite (Martinos Center for Biomedical Imaging, Massachusetts, USA).

*Coherence analysis.* To perform frequency and coherence analyses between the index-finger acceleration and MEG signals of the four movement conditions, continuous data were split into 2048-ms epochs with 1638-ms epoch overlap, leading to frequency resolution of ~0.5 Hz (Bortel and Sovka, 2007). Acceleration corresponding to each epoch was computed at every sample as the Euclidian norm of the three band-passed (1–195 Hz) acceleration signals (Bourguignon et al., 2011). The use of the Euclidian norm of the accelerometer channels allowed us to quantify finger kinematics regardless of hand position. Before the coherence analysis, each epoch of acceleration was normalized by its Euclidian norm. Frequencies of interest, showing consistent coherence across subjects, were applied for source analyses, where cross-spectral density

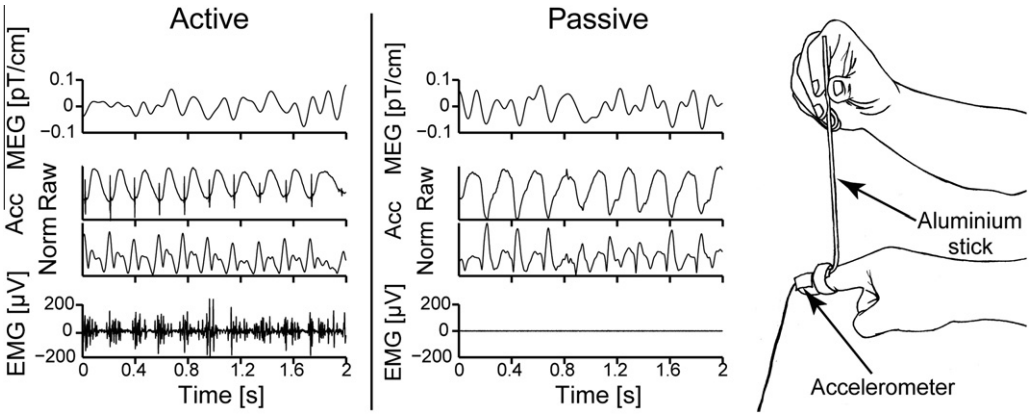


**Fig. 1.** (Left and Middle) Single-trial MEG (top traces), accelerometer (Acc; middle two traces), and EMG signals from a representative subject in *active* (left) and *passive* (right) *no-touch* conditions. The MEG traces, filtered from 1 to 10 Hz, are from a gradiometer channel over the SM1 cortex, contralateral to index-finger movements. For acceleration, both a single axis (Raw) and Euclidian norm (Norm) of the three acceleration signals are presented. EMG signals are from the *flexor carpi radialis* muscle. (Right) Schematic drawing showing the experimental setup for the passive conditions.

matrix was computed between all possible combinations of MEG signals and the Euclidian norm of the acceleration signals (Bourguignon et al., 2011).

*CKC source analysis.* We first estimated noise level at every sensor as the root-mean-square value of the *rest* condition MEG signals (passband 1–195 Hz). We then normalized MEG signals and the MEG forward model coefficients corresponding to each sensor according to this sensor-noise level. Finally, coherence maps at frequencies of interest were produced within the computed source space using the dynamic imaging of coherent sources (DICS) approach with minimum-variance beamformer (Gross et al., 2001; Bourguignon et al., 2011, 2013a).

*SEF source analysis.* The SEF data were filtered through 0.5–40 Hz and analyzed from −100 to 300 ms with respect to stimulus onset. Covariance matrix, computed on unaveraged data in the 30–90 ms range, was used for unit-noise-gain beamformer computation. Beamformer coefficients were further used to compute noise-normalized source power maps (SEF maps) in the 30–90 ms range with respect to stimulus onset. This time range was chosen to match the timing of the main SEF responses.

*Group-level CKC and SEF maps.* Subjects' white matter surfaces were warped to the standard Montreal Neurological Institute (MNI) white matter surface using the spherical morphing procedure implemented in Freesurfer. Then, a morphing map—linearly mapping the cortical surface values in individual subjects' cortex to MNI cortex—was computed using MNE suite, and the results were applied to coherence and SEF maps. To optimize inter-subject comparability, these individual morphed maps were normalized by their maximum value (*i.e.* the node with the maximum value in a normalized morphed map takes value 1). Averaging across subjects yielded a group level map for each condition.

*EMG.* EMG signals were band-pass filtered at 20–195 Hz, with additional notch filters at 50 Hz and its harmonics. For each subject, the mean EMG activity was computed as the difference between root-mean-square of the EMG signals during the movement conditions and the rest condition, which was used to estimate EMG noise level.

*Movement characteristics.* For each subject and movement condition, a parameter quantifying finger-movement regularity was derived from the time-course of the Euclidian norm of the three band-passed (1–195 Hz) acceleration signals. To compute this parameter, power spectrum of the Euclidian norm was computed and smoothed with a 0.1-Hz full-width at half maximum Gaussian kernel. Then, the first peak corresponding to the finger F0 was identified and the regularity parameter was computed as the ratio between the power at F0 and the mean power in the $[2/3 \times F0;\ 3/2 \times F0]$ frequency interval. The value of the regularity parameter increases with sharpness of the F0 peak (*i.e.* with regularity of the movement).

## Statistical analysis

*Movement characteristics.* Both finger F0 and regularity parameter in movement conditions were compared using a two-way 2 (*task*: *active*/*passive*) × 2 (*type*: *touch*/*no-touch*) repeated-measures analysis of variance. Linear spectral densities of hand acceleration between movement conditions were compared using a three-way 2 (*task*: *active*/*passive*) × 2 (*type*: *touch*/*no-touch*) × *n* (frequencies of interest) repeated-measures analysis of variance.

*Sensor-level coherence.* Coherence values at the sensor level (maximal value across all sensors) were assessed under the hypothesis of linear independence at each frequency of interest, taking into account the use of overlapping epochs (Halliday et al., 1995; Bourguignon et al., 2011). Coherence values at the sensor level were considered statistically significant at $p < 0.05$.

*Group-level CKC and SEF map values.* Statistical significance of group-level maps' values was assessed using a non-parametric permutation test. For this purpose, subject- and group-level noise maps were obtained for each condition, either by computing coherence between *rest* MEG signals and acceleration signals of the movement conditions (for CKC), or by using a covariance matrix computed in the baseline (from −90 to −30 ms) range (for SEFs). Under the null hypothesis of no difference between CKC or SEF maps and noise maps, this labeling is arbitrary and can be exchanged prior to group-level map computation (Nichols and Holmes, 2002). To reject the null hypothesis and to assess statistical significance, the sample distribution of the largest difference between the map of

interest and the noise maps was computed from the exhaustive permutation set. Then, all nodes in CKC or SEF maps differing from the noise map more than the 95 percentile of the sample distribution were considered statistically significant (Nichols and Holmes, 2002).

*CKC and SEF source locations.* To assess the inter-condition differences in the cortical source locations, we first excluded in each group-level map all nodes with values significantly different from the map's maximum value ($p < 0.05$ as assessed with a paired t-test across the 15 subjects); the remaining set of nodes can be interpreted as containing the sources of the CKC or SEFs with 95% probability. Differences in cortical source locations between all pairs of conditions were then assessed by the degree of overlap ($\theta$) between two corresponding sets of nodes (one from each map), with $\theta$ defined as the number of nodes belonging to both sets divided by the number of nodes in the smallest set; $\theta$ takes value 1 if the two clusters overlap completely and value 0 if the two clusters do not overlap at all. A low $\theta$ value therefore indicates a source location difference between the two compared conditions.

The statistical significance of $\theta$ was further assessed with a non-parametric permutation test (Nichols and Holmes, 2002). Under the null hypothesis that a common brain area generates both SEFs and all CKC sources, SEFs and CKC (*touch*/*no-touch*; *active*/*passive*; frequencies of interest) are arbitrary labels for the maps, and the statistical significance of $\theta$ can be assessed by comparison with the distribution of values obtained when the labels are permuted (Nichols and Holmes, 2002). Accordingly, the sample distribution of the minimal—across condition pairs—$\theta$ value was computed from 10.000 different permutations and a threshold for $\theta$ at $p < 0.05$ was computed as the 5 percentile of this sample distribution (Nichols and Holmes, 2002).

*Strength of CKC.* Possible differences in strength of coherence between movement conditions were compared using a three-way 2 (*task*: *active*/*passive*) × 2 (*type*: *touch*/*no-touch*) × *n* (frequencies of interest) repeated-measures analysis of variance. The dependent variable was the subjects' individual coherence value at the node with the maximum value in the group-level map.

*EMG.* The EMG activity during movement and *rest* conditions was compared using a one-way repeated-measures analysis of variance (4 conditions: *active-touch*, *active-no-touch*, *passive-touch*, *passive-no-touch*).

## RESULTS

Fig. 1 shows 2-s epochs of a representative subject's MEG, acceleration, and EMG signals during both *active* (left panel) and *passive* (right panel) movements. The main frequencies of the acceleration and MEG are the same, and visible already in the raw signals. During the *active* movement, EMG bursts are time-locked to acceleration peaks whereas no EMG activity is present during the *passive* movement.

Fig. 2 shows linear spectral densities of hand acceleration in each condition, with individual subjects' traces superimposed, and examples of the magnitude (Euclidean norm) of hand acceleration from a single subject. Acceleration peak is evident at each movement cycle, and it was especially strong in *touch* conditions where the acceleration changed abruptly. The spectral densities were very similar across subjects, but higher at F0 than at F1 in all conditions (effect of *frequency*, $F_{1,14} = 178$, $p < 0.001$), and higher in *no-touch* than *touch* conditions (effect of *type*, $F_{1,14} = 47.8$, $p < 0.001$), with an interaction between the movement *frequency* and *type* ($F_{1,14} = 68.4$, $p < 0.001$). The spectral densities were always higher in *no-touch* than *touch* conditions ($p < 0.05$–$0.001$), and at F0 than F1 ($p < 0.001$). No main effect was detected for movement *task* (*active vs. passive*). However, the movement *task*

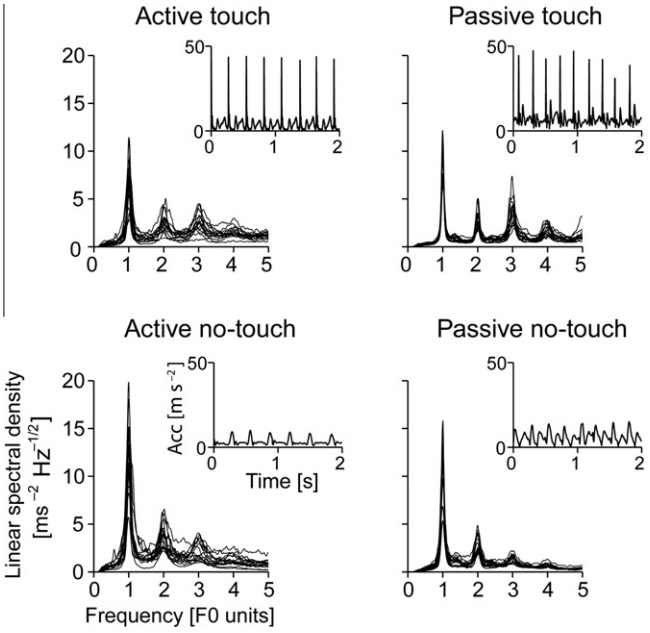


**Fig. 2.** Linear spectral densities of hand acceleration as a function of frequency normalized according to individual movement frequency (F0); the superimposed traces are from different subjects ($N = 15$) and data are given for all conditions. The inserts depict 2-s epochs of the Euclidian norm (Acc) of hand acceleration for each condition.

**Table 1.** MNI coordinates (*x*, *y*, and *z*) of the node with maximum value in each group-level CKC map in movement conditions and source-power SEF map, and the corresponding (mean ± SEM) coherence and linear spectral density values across all subjects at movement frequency (F0) and its first harmonic (F1)

| Frequency | Condition | MNI coordinates | | | Coherence | Linear spectral density ($ms^{-2}\,Hz^{-1/2}$) |
|---|---|---|---|---|---|---|
| F0 | *active-touch* | −43 | −32 | 65 | 0.16 ± 0.04 | 7.2 ± 0.7 |
| | *active-no-touch* | −41 | −29 | 62 | 0.19 ± 0.05 | 12.4 ± 1.0 |
| | *passive-touch* | −51 | −29 | 55 | 0.22 ± 0.05 | 9.5 ± 0.5 |
| | *passive-no-touch* | −46 | −33 | 62 | 0.17 ± 0.04 | 11.6 ± 0.9 |
| F1 | *active-touch* | −42 | −28 | 64 | 0.25 ± 0.06 | 2.7 ± 0.3 |
| | *active-no-touch* | −44 | −25 | 60 | 0.21 ± 0.04 | 4.2 ± 0.4 |
| | *passive-touch* | −44 | −25 | 60 | 0.36 ± 0.06 | 3.0 ± 0.3 |
| | *passive-no-touch* | −44 | −25 | 60 | 0.39 ± 0.05 | 2.9 ± 0.3 |
| SEFs | | −40 | −16 | 46 | | |

interacted significantly with the movement *type* ($F_{1,14} = 14.1$, $p < 0.01$); the spectral density was higher in *passive task* than *active task* during *touch* conditions ($6.24 \pm 0.37\ ms^{-2}\ Hz^{-1/2}$ *vs.* $4.98 \pm 0.44\ ms^{-2}\,Hz^{-1/2}$, $p < 0.05$), but not during the *no-touch* conditions. Table 1 shows group means of the linear spectral densities.

### Movement characteristics

Frequency of finger movement (Table 2) did not differ significantly between movement *tasks* ($F_{1,14} = 0.40$, $p = 0.54$) or *types* ($F_{1,14} = 1.09$, $p = 0.31$), even though *task* and *type* interacted significantly ($F_{1,14} = 13.50$, $p < 0.01$). The analysis of variance comparing the regularity of index-finger movements revealed a significant effect of *task* ($F_{1,14} = 11.1$, $p < 0.01$), and no effect of *type* ($F_{1,14} = 0.0124$, $p = 0.91$) nor interaction ($F_{1,14} = 0.0764$, $p = 0.79$). The regularity-parameter (Table 2) averaged across subjects and *type* showed that movement was more regular ($p < 0.01$) in *passive* task (regularity-parameter: 3.3 ± 0.2) than in *active* task (regularity-parameter: 2.5 ± 0.1).

### Sensor level coherence

All subjects performed all tasks with no difficulties. Statistically significant ($p < 0.05$) coherence was found between the acceleration signals and MEG signals during all four *active* and *passive* conditions both at the F0 and its F1, except in two subjects in *active-touch* at F0. Thus F0 and F1 were used as frequencies of interest in the source analysis, resulting in total of eight CKC sources (4 conditions × 2 frequencies of interest). Fig. 3 shows subjects' individual coherence spectra between MEG and hand acceleration.

### CKC and SEF source locations

Fig. 4 shows CKC and SEF group-level maps that all showed statistically significant values. All eight CKC sources were located in the hand area of the contralateral SM1 cortex, with no spatial differences

**Table 2.** Mean ± SEM movement frequency and the regularity parameter of the finger movement during four conditions

| Subject | Movement frequency | | | | Regularity parameter | | | |
|---|---|---|---|---|---|---|---|---|
| | *Active* | | *Passive* | | *Active* | | *Passive* | |
| | *touch* | *no-touch* | *touch* | *no-touch* | *touch* | *no-touch* | *touch* | *no-touch* |
| 1 | 3.4 | 3.4 | 4.9 | 4.4 | 1.5 | 2.4 | 3.8 | 2.7 |
| 2 | 4.4 | 3.9 | 3.9 | 2.9 | 3.1 | 2.5 | 2.7 | 2.7 |
| 3 | 3.4 | 3.4 | 4.4 | 3.9 | 3.2 | 2.8 | 4.2 | 2.7 |
| 4 | 4.4 | 4.4 | 4.4 | 4.4 | 2.4 | 2.1 | 4.9 | 4.0 |
| 5 | 3.4 | 4.4 | 4.4 | 4.4 | 1.9 | 2.4 | 2.3 | 2.9 |
| 6 | 3.4 | 3.4 | 4.4 | 4.4 | 2.0 | 3.3 | 4.0 | 3.7 |
| 7 | 4.4 | 4.4 | 4.4 | 4.4 | 2.1 | 2.4 | 2.6 | 3.1 |
| 8 | 3.4 | 3.9 | 4.4 | 4.4 | 3.6 | 3.0 | 2.7 | 3.1 |
| 9 | 3.9 | 3.9 | 4.4 | 4.4 | 2.4 | 3.5 | 2.6 | 3.1 |
| 10 | 4.9 | 5.4 | 4.4 | 4.4 | 2.1 | 1.3 | 3.6 | 3.5 |
| 11 | 4.9 | 4.9 | 4.4 | 4.4 | 2.4 | 2.4 | 5.5 | 4.7 |
| 12 | 3.4 | 3.4 | 3.4 | 2.9 | 3.4 | 2.8 | 3.3 | 3.2 |
| 13 | 4.4 | 4.4 | 3.4 | 2.9 | 2.6 | 2.2 | 4.0 | 3.9 |
| 14 | 3.9 | 3.9 | 3.9 | 3.9 | 2.5 | 3.5 | 3.9 | 4.4 |
| 15 | 3.4 | 2.9 | 3.9 | 3.4 | 3.1 | 2.3 | 1.8 | 3.2 |
| Mean ± SEM | 3.9 ± 0.2 | 4.0 ± 0.2 | 4.2 ± 0.1 | 4.0 ± 0.2 | 2.6 ± 0.2 | 2.6 ± 0.2 | 3.5 ± 0.3** | 3.4 ± 0.2** |

** $p < 0.01$ between *active* and *passive* tasks.

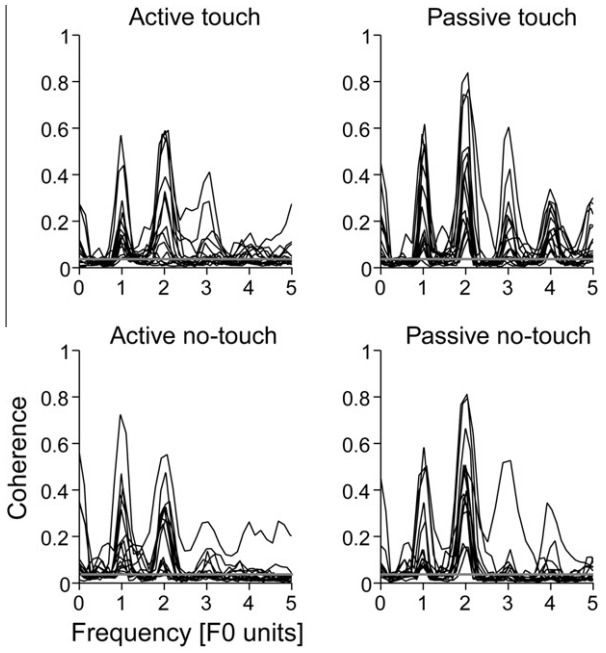


**Fig. 3.** Individual coherence spectra between MEG and hand acceleration in each condition. Each trace represents the coherence level for a single subject as a function of the frequency normalized by the subjects' movement frequency (F0). Horizontal line shows the threshold for statistical significance ($p < 0.05$).

between the four movement conditions (*active-touch*, *active-no-touch*, *passive-touch*, *passive-no-touch*) at F0 and F1. The CKC maps showed maximum value in the post-central gyrus, *i.e.*, the S1 cortex but covered also the precentral gyrus, *i.e.*, the M1 cortex, except in *passive-touch* and *passive-no-touch* at F1.

The CKC source maps did not overlap significantly ($p < 0.05$) with the SEF source map, except for *active-no-touch-F0* ($p = 0.07$) and *passive-no-touch-F0* ($p = 0.24$) conditions. The SEF source was located at the anterior wall of the post-central gyrus (area 3b of S1 cortex).

Table 1 provides MNI coordinates of the node with the maximum value in each CKC and SEF map.

### Strength of CKC

Strength of CKC was affected by *task* (*active vs. passive*, $F_{1,14} = 8.85$ $p < 0.01$) and *frequency* (F0 *vs.* F1, $F_{1,14} = 16.25$, $p < 0.01$) with an interaction between them ($F_{1,14} = 7.29$, $p < 0.05$), whereas movement *type* (*touch vs. no-touch*) had no effect. The mean CKC level across the movement *types* was 118% ($p < 0.001$), 63% ($p < 0.01$) and 94% ($p < 0.001$) higher during *passive* tasks at F1 when compared with *active-F0*, *active-F1* and *passive-F0*, respectively. Table 1 shows the CKC strength for all movement *tasks*, *types*, and response *frequencies*.

### EMG

EMG level measured during passive conditions did not differ from the noise level. However, the EMG level was higher during *active* conditions (*touch* or *no-touch*) than during *passive* (*touch* or *no-touch*) or *rest* conditions ($p < 0.01$) for both the extensor ($F_{3,42} = 33.09$, $p < 0.001$) and flexor ($F_{3,42} = 10.74$, $p < 0.001$) muscles, whereas it did not differ within the *active* conditions, nor within the *passive* conditions (Fig. 5).

## DISCUSSION

This study demonstrates that coherence between MEG signals and index-finger acceleration can be observed during *passive* index movements with similar coherence levels and neural generators than those obtained during *active* index movements. The coherence peaked at F0 and F1, in line with previous studies using *active* hand-movements (Jerbi et al., 2007; Bourguignon et al., 2011, 2012; Piitulainen et al., 2013), and was about 63% stronger during *passive* than *active* finger movements at F1, but equally strong at F0, with no effect of movement *type (touch vs. no-touch*). The main sources of the coherent signals were at the hand area of the SM1 cortex, contralateral to finger movements, with no statistically significant spatial difference between sources for *active* and *passive* movements. Sources of SEFs to tactile stimulation of the index finger were distinct from most of the CKC sources, and they were located in the anterior wall of the post-central gyrus at the S1 finger area, in agreement with earlier studies (for a review, see (Hari and Forss, 1999)).

### Motor versus somatosensory contribution to CKC

Our results imply that the active motor contribution to CKC is minimal, and that the coherence strongly reflects somatosensory input to the SM1 cortex. Indeed, all *active* and *passive* finger flexion–extension tasks resulted in significant CKC, at both F0 and F1, without any consistent spatial differences across conditions, and with no systematic posterior shift of source locations for passive movements with respect to *active* ones. These results confirm that the SM1 cortex is the main generator of CKC, although they cannot conclude whether only the S1 or only M1 cortex, or both of these neighboring areas are involved.

All SM1 areas receiving proprioceptive input are potential candidates for CKC generation. Areas 1 and 3b of the S1 cortex receive mainly cutaneous tactile inputs (Kaas 1983) whereas areas 3a and 2 receive proprioceptive inputs (from joint and muscle receptors) and respond to joint movements (Burchfiel and Duffy, 1972; Schwarz et al., 1973) as well as to passive stretching of muscles (Lucier et al., 1975). The human M1 cortex also receives proprioceptive feedback during both active and passive hand movements while it remains silent during tactile stimulation (Goldring and Ratcheson, 1972). These findings and the currently observed significant CKC during both *active* and *passive* finger movements suggest generation of the CKC at hand S1 and M1 cortices by proprioceptive feedback. The proprioceptive predominance is further supported by the lack of significant overlap between the CKC and SEF source maps; SEFs are known to mainly reflect

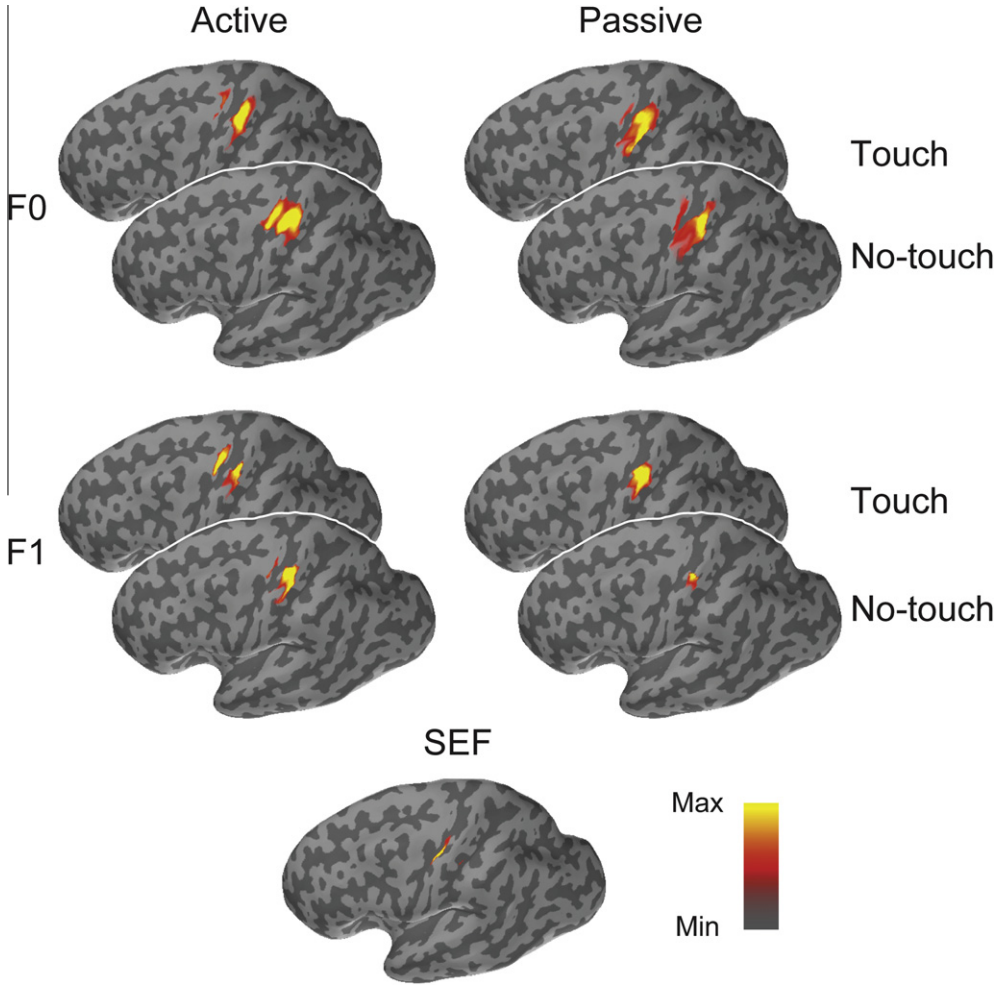


**Fig. 4.** Left-hemisphere group-level CKC and SEF maps. The color-code represents the group-level maps' values obtained as described in the methods. All nodes significantly different from the node with the maximum value are hidden; the adaptive color scale matches the range of remaining values (min and max are different for each condition). Maximum values of the CKC maps co-localize with the anatomical SM1 hand area.

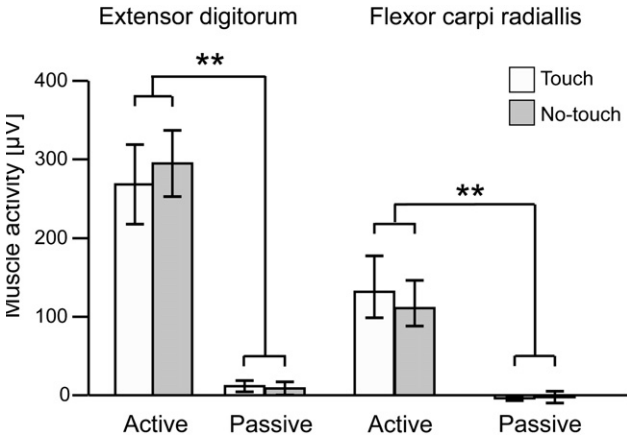


**Fig. 5.** Mean ± SEM values for EMG RMS amplitudes computed as the differences from the rest-condition values, given separately for *extensor digitorum* and *flexor carpi radialis* muscles during *active* and *passive* movements. Values in the passive condition did not differ from the zero (rest) level. $^{**}p < 0.01$.

cutaneous tactile afferent input to area 3b (and probably 1) of the S1 cortex.

Although most somatosensory afferents project in monkey via the ventral posterior thalamus to the S1 cortex (Kaas 1993), and not directly to the M1 cortex (Huffman and Krubitzer, 2001), M1 does receive input from proprioceptors (mainly muscle spindles) at similar short latencies (5–10 ms) as area 3a of the S1 cortex (Devanandan and Heath, 1975; Lucier et al., 1975). Thus the M1 cortex likely receives direct proprioceptive input in addition to cortico-cortical connections via somatosensory areas 1 and 2 (Jones et al., 1978). Moreover, vibration of a tendon, known to activate muscle spindles similarly as does muscle stretch (Burke et al., 1976; Roll and Vedel, 1982; Gandevia 1985), activated in a PET study more strongly the M1 cortex than the S1 cortex (Naito et al., 1999; Naito and Ehrsson, 2001). In light of these studies and our results, CKC likely originates from proprioceptive feedback to the SM1 cortex, although we cannot conclude whether M1, S1, or both cortices are involved. For the current

fast finger movements, we were not able to determine consistent delays between the acceleration and MEG signals and thus could not estimate latencies for the sensory input.

### Effect of concomitant tactile stimulation

Most CKC sources were spatially separated from sources of SEFs to tactile stimulation. Moreover, cutaneous input from the tip of index finger to the S1 cortex did not substantially contribute to CKC, since touching the table (*touch vs. no-touch* condition) with the fingertip did not have any significant effect on coherence strength nor on the location of the main CKC sources.

This result contradicts a previous finding of stronger CKC during *touch* than *no-touch* condition in a hand flexion–extension task (Bourguignon et al., 2012). However, the CKC level can be affected by several factors, such as movement rate and steadiness, range of motion, and the muscles involved. The difference between the studies might be due to different motor tasks (hand versus index-finger movements, all fingers touching the thumb versus index finger touching a table at each movement cycle), which makes direct comparison of the CKC level difficult. Nevertheless, the current results are in line with some other previous findings. First, fMRI shows similar activity patterns in a finger–thumb opposition task independently whether fingers are touching or not touching the thumb (Jansma et al., 1998). Second, somatosensory-evoked potentials (SEPs) recorded from the scalp to passive finger movements are preserved even when joint and cutaneous afferents are blocked by ischemic anesthesia of finger while muscle spindle afferents remain intact; the SEPs disappeared only when the anesthesia was extended to the forearm muscles and palm, thereby blocking muscle spindle afferents (Mima et al., 1996). These results could in part be explained by ‘‘gating’’ of cutaneous inputs during both active and passive movements, as is also indicated by the weaker perceived intensities of cutaneous stimuli (Milne et al., 1988), higher perceptual thresholds (Angel and Malenka, 1982), and reduced SEPs to electrical stimulation of digital nerves of thumb (Rushton et al., 1981) and median nerve (Jones et al., 1989) both during active and passive movements. We thus consider the concomitant cutaneous stimulation during passive movements have negligible effect on the CKC measured in our current setting.

### Coherence at F0 and F1

During *active* repetitive flexion–extension finger movements, the SM1 cortex can be coherent with the movement kinematics both because of rhythmically generated motor commands and rhythmic proprioceptive feedback from the muscles. However, the muscles were silent during passive finger movements, and thus the coherence mainly reflected somatosensory, likely the proprioceptive feedback. The M1 and S1 cortices are located at opposite sides of the central sulcus, and thus cancelation of their opposite currents at some stages of the movement cycle may have affected to the observed signal strengths. Unfortunately, we are not able to make any further conclusion on the basis of our present data whether the effect is different for F0 and F1.

During passive, but not active movements, the coherence was stronger at F1 than F0. Although the mechanisms involved in F1 coherence are still unsettled and need further investigation, one plausible explanation for the F0 *vs.* F1 difference derives from the slightly different kinematics of the passive and active movements. Although the mean movement rate did not differ between the conditions, the rate was by a third more regular for the *passive* movements performed by an experienced investigator than for the *active* movements. The enhanced movement regularity will in turn strengthen the observed coherence between acceleration and MEG signals because time variability leads to phase variability that is proportional to the frequency and thus twice more important at F1 than at F0. Despite the higher regularity of passive than active movements, the power of the hand acceleration both at F0 and F1 was similar between the *active* and *passive* conditions. Somewhat surprisingly, the power of hand acceleration was significantly higher both at F0 and F1 in *no-touch* conditions compared with *touch* conditions, likely due to power spread to the higher frequencies because of the fast deceleration of the finger when hitting the table during the *touch* conditions. Despite these significant differences in the kinematics, the coherence strength did not differ between the *touch* and *no-touch conditions*.

The functional significance of CKC at F1 remains unclear. It may not represent just the harmonic of the F0 coherence but rather a response to proprioceptive feedback from both the flexor and extensor muscles occurring altogether twice during each movement cycle. For active movements, the respective efferent motor commands occur twice during each active movement cycle, and thus could, in principle, also contribute to coherence at F1. However, our findings demonstrate a dominant role of the sensory feedback in the generation of the CKC.

## CONCLUSIONS

We have shown that the acceleration of index finger is coherent with the contralateral SM1 cortex during both *active* and *passive* index-finger movements, with similar location of the main generator in both conditions. CKC seems to be mainly driven by proprioceptive feedback, with no major indication in our data of the effect of cutaneous input.

## AUTHOR CONTRIBUTIONS

All authors participated in the conception and design of the studies. H.P. and M.B. conducted the measurements. All the authors participated in the interpretation of the data. Original draft was prepared by H.P. and M.B. but the five authors critically revised the manuscript before approving the final version.

## DISCLOSURE

No conflicts of interest, financial or otherwise, are declared by the authors. All authors have approved the final article.

*Acknowledgments—This work was supported by the Academy of Finland (National Centers of Excellence Program 2006–2011, Grant #129678 and Grant 131483 to Riitta Hari), the SalWe Research Program for Mind and Body (Tekes – the Finnish Funding Agency for Technology and Innovation Grant 1104/10), the ERC Advanced Grant (#232946 to Riitta Hari), and the "Brains Back to Brussels" grant to Veikko Jousmäki from the Institut d'Encouragement de la Recherche Scientifique et de l'Innovation de Bruxelles (Brussels, Belgium), the Fonds de la Recherche Scientifique (FRS-FNRS, Belgium, Research Convention 3.4611.08). Mathieu Bourguignon received a research grant from the FRIA (FRS-FNRS, Belgium). Xavier De Tiège is Clinicien-Chercheur Spécialiste at the FRS-FNRS, Belgium.*

*We thank Helge Kainulainen and Ronny Schreiber at the Brain Research Unit (School of Science, Aalto University, Espoo, Finland) for technical support, and Kati Karvonen for illustrations.*

## REFERENCES

Alary F, Simoẽs C, Jousmäki V, Forss N, Hari R (2002) Cortical activation associated with passive movements of the human index finger: an MEG study. NeuroImage 15:691–696.

Angel RW, Malenka RC (1982) Velocity-dependent suppression of cutaneous sensitivity during movement. Exp Neurol 77:266–274.

Bortel R, Sovka P (2007) Approximation of statistical distribution of magnitude squared coherence estimated with segment overlapping. Signal Process 87:1100–1117.

Bourguignon M, De Tiège X, Op de Beeck M, Pirotte B, Van Bogaert P, Goldman S, Hari R, Jousmäki V (2011) Functional motor–cortex mapping using corticokinematic coherence. NeuroImage 55:1475–1479.

Bourguignon M, Jousmäki V, Op de Beeck M, Van Bogaert P, Goldman S, De Tiège X (2012) Neuronal network coherent with hand kinematics during fast repetitive hand movements. NeuroImage 59:1684–1691.

Bourguignon M, De Tiège X, Op de Beeck M, Ligot N, Paquier P, Van Bogaert P, Goldman S, Hari R, Jousmäki V (2013a) The pace of prosodic phrasing couples the listener's cortex to the reader's voice. Hum Brain Mapp 34:314–326.

Bourguignon M, De Tiège X, Op de Beeck M, Van Bogaert P, Goldman S, Jousmäki V, Hari R (2013b) Primary motor cortex and cerebellum are coupled with the kinematics of observed hand movements. NeuroImage 66:500–507.

Burchfiel JL, Duffy FH (1972) Muscle afferent input to single cells in primate somatosensory cortex. Brain Res 45:241–246.

Burke D, Hagbarth KE, Lofstedt L, Wallin BG (1976) The responses of human muscle spindle endings to vibration of non-contracting muscles. J Physiol 261:673–693.

Devanandan MS, Heath PD (1975) Proceedings: a short latency pathway from forearm nerves to area 4 of the baboon's cerebral cortex. J Physiol 248:43P–44P.

Gandevia SC (1985) Illusory movements produced by electrical stimulation of low-threshold muscle afferents from the hand. Brain 108(Pt 4):965–981.

Goldring S, Ratcheson R (1972) Human motor cortex: sensory input data from single neuron recordings. Science 175:1493–1495.

Gross J, Kujala J, Hämäläinen M, Timmermann L, Schnitzler A, Salmelin R (2001) Dynamic imaging of coherent sources: studying neural interactions in the human brain. Proc Natl Acad Sci U S A 98:694–699.

Halliday DM, Rosenberg JR, Amjad AM, Breeze P, Conway BA, Farmer SF (1995) A framework for the analysis of mixed time series/point process data–theory and application to the study of physiological tremor, single motor unit discharges and electromyograms. Prog Biophys Mol Biol 64:237–278.

Hari R, Forss N (1999) Magnetoencephalography in the study of human somatosensory cortical processing. Philos Trans R Soc Lond B Biol Sci 354:1145–1154.

Huffman KJ, Krubitzer L (2001) Thalamo-cortical connections of areas 3a and M1 in marmoset monkeys. J Comp Neurol 435:291–310.

Jansma JM, Ramsey NF, Kahn RS (1998) Tactile stimulation during finger opposition does not contribute to 3D fMRI brain activity pattern. Neuroreport 9:501–505.

Jerbi K, Lachaux JP, N'Diaye K, Pantazis D, Leahy RM, Garnero L, Baillet S (2007) Coherent neural representation of hand speed in humans revealed by MEG imaging. Proc Natl Acad Sci U S A 104:7676–7681.

Jones EG, Coulter JD, Hendry SH (1978) Intracortical connectivity of architectonic fields in the somatic sensory, motor and parietal cortex of monkeys. J Comp Neurol 181:291–347.

Jones SJ, Halonen JP, Shawkat F (1989) Centrifugal and centripetal mechanisms involved in the 'gating' of cortical SEPs during movement. Electroencephalogr Clin Neurophysiol 74:36–45.

Kaas JH (1993) The functional organization of somatosensory cortex in primates. Ann Anat 175:509–518.

Kaas JH (1983) What, if anything, is SI? Organization of first somatosensory area of cortex. Physiol Rev 63:206–231.

Kocak M, Ulmer JL, Sahin Ugurel M, Gaggl W, Prost RW (2009) Motor homunculus: passive mapping in healthy volunteers by using functional MR imaging – initial results. Radiology 251:485–492.

Lucier GE, Ruegg DC, Wiesendanger M (1975) Responses of neurones in motor cortex and in area 3A to controlled stretches of forelimb muscles in cebus monkeys. J Physiol 251:833–853.

Milne RJ, Aniss AM, Kay NE, Gandevia SC (1988) Reduction in perceived intensity of cutaneous stimuli during movement: a quantitative study. Exp Brain Res 70:569–576.

Mima T, Terada K, Maekawa M, Nagamine T, Ikeda A, Shibasaki H (1996) Somatosensory evoked potentials following proprioceptive stimulation of finger in man. Exp Brain Res 111:233–245.

Mima T, Sadato N, Yazawa S, Hanakawa T, Fukuyama H, Yonekura Y, Shibasaki H (1999) Brain structures related to active and passive finger movements in man. Brain 122(Pt. 10):1989–1997.

Naito E, Ehrsson HH (2001) Kinesthetic illusion of wrist movement activates motor-related areas. Neuroreport 12:3805–3809.

Naito E, Ehrsson HH, Geyer S, Zilles K, Roland PE (1999) Illusory arm movements activate cortical motor areas: a positron emission tomography study. J Neurosci 19:6134–6144.

Nichols TE, Holmes AP (2002) Nonparametric permutation tests for functional neuroimaging: a primer with examples. Hum Brain Mapp 15:1–25.

Oldfield RC (1971) The assessment and analysis of handedness: the Edinburgh inventory. Neuropsychologia 9:97–113.

Piitulainen H, Bourguignon M, De Tiège X, Hari R, Jousmäki V (2013) Coherence between magnetoencephalography and hand-action-related acceleration, force, pressure, and electromyogram. NeuroImage 72:83–90.

Reddy H, Floyer A, Donaghy M, Matthews PM (2001) Altered cortical activation with finger movement after peripheral denervation: comparison of active and passive tasks. Exp Brain Res 138:484–491.

Roll JP, Vedel JP (1982) Kinaesthetic role of muscle afferents in man, studied by tendon vibration and microneurography. Exp Brain Res 47:177–190.

Rushton DN, Rothwell JC, Craggs MD (1981) Gating of somatosensory evoked potentials during different kinds of movement in man. Brain 104:465–491.

Schwarz DW, Deecke L, Fredrickson JM (1973) Cortical projection of group I muscle afferents to areas 2, 3a, and the vestibular field in the rhesus monkey. Exp Brain Res 17:516–526.

Taulu S, Kajola M, Simola J (2004) Suppression of interference and artifacts by the signal space separation method. Brain Topogr 16:269–275.

Weiller C, Jüptner M, Fellows S, Rijntjes M, Leonhardt G, Kiebel S, Müller S, Diener HC, Thilmann AF (1996) Brain representation of active and passive movements. NeuroImage 4:105–110.

Woldag H, Waldmann G, Schubert M, Oertel U, Maess B, Friederici A, Hummelsheim H (2003) Cortical neuromagnetic fields evoked by voluntary and passive hand movements in healthy adults. J Clin Neurophysiol 20:94–101.

Xiang J, Kakigi R, Hoshiyama M, Kaneoke Y, Naka D, Takeshima Y, Koyama S (1997a) Somatosensory evoked magnetic fields and potentials following passive toe movement in humans. Electroencephalogr Clin Neurophysiol 104:393–401.

Xiang J, Hoshiyama M, Koyama S, Kaneoke Y, Suzuki H, Watanabe S, Naka D, Kakigi R (1997b) Somatosensory evoked magnetic fields following passive finger movement. Brain Res Cogn Brain Res 6:73–82.

*(Accepted 3 February 2013)*
*(Available online 10 February 2013)*